Molecular diffusion in liquid crystals and chiral discrimination. II. Model calculations

Diego Frezzato[a], Claudio Zannoni[b], Giorgio J. Moro[a*]

[a] *Dipartimento di Scienze Chimiche and INSTM, Università di Padova, via Marzolo 1, I-35131 Padova, Italy*

[b] *Dipartimento di Chimica Fisica ed Inorganica and INSTM, Viale Risorgimento 4, I-40136, Bologna, Italy*

[*]To whom correspondence should be addressed. fax: +39 0498275239; E-mail: giorgio.moro@unipd.it

Abstract

We perform model calculations of the macroscopic diffusion coefficient for a solute moving in a chiral nematic (cholesteric) liquid crystal (LC) phase applying the methodology developed in D. Frezzato et al., *J. Chem. Phys.* **122**, 164904 (2005). Three types of solutes with different features are studied: ellipsoid (roto-translational coupling (RTC) absent), bent-rod (RTC present) and two-blade propeller (with RTC and chiral shape). For each prototype molecule we estimate the effect of cholesteric helix pitch and local order on the diffusion along the helix axis. For the ellipsoidal particle we find that translational diffusion is slowed down by rotation around the short axis. For the chiral solute we show that the enantiomer with shape chirality opposite to that of the LC phase is slowed down more than the other. This provides a proof of principle of the possibility of separating the two enantiomers via transport in a suitable chiral medium.

1 Introduction

In a previous work [1], from now on denoted as I, we have developed the theoretical tools to evaluate the macroscopic diffusion coefficients in liquids and liquid crystals, namely in uniformly aligned and twisted nematic (or proper cholesteric) phases [2]. The method was based on the calculation of the long-time behavior of the molecular mean-squared-displacement by accounting for the full roto-translational dynamics in the overdamped regime of motion according to the Fokker-Planck-Smoluchowski model [3]. In particular, we were interested in investigating how the roto-translational (RT) coupling in the diffusion matrix (at microscopic level) affects the macroscopic transport in the various phases. Differently from previously available theories, that treated only diffusion in isotropic media [4], our analysis has considered in detail anisotropic phases, where the local orientational ordering is a further feature influencing (and possibly controlling) the macroscopic transport.

The work in I was stimulated by the challenge of assessing the possibility of employing twisted nematics to separate the enantiomers of a chiral compound on the basis of their different diffusion properties. This idea is based on the fact that the friction tensor [5, 6], and the corresponding diffusion tensor $\mathbf{D}^{MF}$ as well (here "MF" denotes a reference frame attached to the molecule), differentiates the enantiomeric forms of a chiral compound: while the diagonal translational and rotational blocks of $\mathbf{D}^{MF}$ are unaffected by inversion, the off-diagonal roto-translational blocks change sign. Moreover the medium itself is intrinsically chiral because of the helical twist of the director, and could discriminate the enantiomers through their different rotational motion coupled to translation.

It is worth noticing that the separation between shape enantiomers in dynamic conditions has been recently put forward as a viable technique, albeit in a rather different context [7]. It has been demonstrated that enantiomers of mesoscopic particles can be discriminated by exploiting a steady-state microflow of the embedding fluid in micro-fabricated devices. Spatial separation emerges from the coupling between the microflow of the fluid (with spatially variable vorticity due to the constraints imposed by the geometry of the device) and the stochastic roto-translational diffusion of the particle; the chiral discrimination is due to the existence of several attractors in the phase-space of the particle dynamics, with different

stability for the two enantiomers. On the contrary, in our work we focus on particles of molecular dimensions, and refer to dynamics of the single molecule occurring in a chiral fluid (the twisted phase) at thermal equilibrium. The phase itself provides directly the "environmental" chirality probed at the molecular length-scale, which is responsible for enantiomeric discrimination (and possible separation).

Since the practical implementation would require a significant differentiation between the two enantiomers, our purpose is to estimate (with the help of the already developed tools [1]) the magnitude of the diffusion coefficient for simple "archetype" chiral molecules and for reasonable parameterizations of the chiral phase. This constitutes the main issue of the present work devoted to model calculation.

In particular we focus on the *m*acroscopic *t*ransport coefficient, $D_{mt}(\mathbf{u}_{hx})$, along the helical axis, $\mathbf{u}_{hx}$, of the phase. Anyway, some intermediate steps are required to achieve a basic view before exploring the molecular chirality feature. We proceed by selecting some archetype molecules of growing complexity: 1) an ellipsoidal molecule possessing no RT coupling in the roto-translational diffusion matrix $\mathbf{D}^{MF}$; 2) an a-chiral bent-rod molecule possessing RT coupling; 3) a propeller-like molecule possessing both RT coupling in the matrix $\mathbf{D}^{MF}$ and shape chirality. Our aim is to answer the following questions by directly looking at the profile of $D_{mt}(\mathbf{u}_{hx})$ versus the increasing pitch of the phase (i.e, passing from a strongly twisted phase to a uniform nematic): i) How does the strength of local orientational potential and thus the local order affect the macroscopic translational diffusion? ii) Since the twist of the director on the short length-scale generates local biaxiality of the nematic-like phase, can such biaxiality induce significant effects on the macroscopic diffusion? iii) Which is the effect of the hydrodynamical RT coupling (in the $\mathbf{D}^{MF}$ matrix) on the long-range diffusion? Then, our final question is: iv) Can shape enantiomers be distinguished by the translational diffusion process?

Along these lines, the paper is structured as follows. In section 2 we summarize the methodology presented in I for the evaluation of the macroscopic transport coefficient in cholesteric phases, by specifying the leading contributions to migration along the helical axis $\mathbf{u}_{hx}$. Technical details required to compute $D_{mt}(\mathbf{u}_{hx})$ are described in section 3 and

in the EPAPS Supporting Information [8]. In section 4 we outline the model calculations. The answer to questions i) and ii) is given in section 5 by considering the simplest model system, i.e., the ellipsoidal molecule. For a clear answer to question iii), in section 6 we take into account the bent-rod molecule as the simplest object possessing hydrodynamical RT coupling without chirality. Question iv) is faced in section 7 by considering the propeller-like molecules. The last section is devoted to the main conclusions.

2 Macroscopic diffusion in cholesteric phases

In part I we have treated the problem of evaluating the macroscopic transport coefficient monitored along a generic direction $\mathbf{u}$, $D_{mt}(\mathbf{u})$, in isotropic, nematic, and twisted nematic/cholesteric phases. In this section we review such methodology for the latter situation, and specialize it to the case of molecular migration monitored along the helical axis of the phase denoted by $\mathbf{u}_{hx}$.

First, we recall (see figure 1) the systems of axes employed in part I to describe statics and dynamics in a cholesteric sample modeled as a twisted nematic phase. We start by introducing a Molecular Frame attached to a moving probe-molecule, MF= $(\mathbf{x}^{MF}, \mathbf{y}^{MF}, \mathbf{z}^{MF})$. The unique restriction about the choice of MF regards its origin, which should be located at the so-called Center of Diffusion (CD) of the molecule in order to simplify the formal treatment (as clarified in the following), while the orientation of the MF axes can be arbitrarily chosen. Then we introduce a Laboratory Frame, LF= $(\mathbf{x}^{LF}, \mathbf{y}^{LF}, \mathbf{z}^{LF})$, with $\mathbf{z}^{LF} = \mathbf{u}_{hx}$ along the helical axis, while $\mathbf{x}^{LF}$ is taken collinear to the director at the origin of the frame (which can be arbitrarily located). With reference to LF, the variable that specifies the instantaneous molecular state is $Q = (\mathbf{r}, \Omega)$, where $\mathbf{r} = (x, y, z)$ are the coordinates of the MF center and Ω is the set of Euler angles defined according to Rose's convention [11] for the transformation LF$\rightarrow$MF.

From the long-time limit of the molecular mean-squared displacements, the coefficient

$D_{mt}(\mathbf{u})$ is evaluated as

$$D_{mt}(\mathbf{u}) \equiv \lim_{t\to\infty} \overline{[\mathbf{u}\cdot\Delta\mathbf{r}(t)]^2/2t} \tag{1}$$

where the time evolution of $\Delta\mathbf{r}(t)$ is determined by the roto-translational (RT) dynamics of the probe. The RT motion has been modeled as a diffusive process in the overdamped regime [3], with $(\mathbf{r},\Omega) = Q$ the relevant stochastic variables. The input to the modeling consists of i) the equilibrium distribution function $p_{eq}(Q)$, and ii) the *microscopic* friction tensor for the RT small-steps dynamics in the local viscous environment.

In order to deal with a position invariant distribution, a further reference frame, namely the Director Frame DF= $(\mathbf{x}^{DF},\mathbf{y}^{DF},\mathbf{z}^{DF})$, has been introduced. The axes of DF are position-dependent: the z-axis is still collinear to the helical axis (as for LF), but the x-axis constantly points along the local director at the actual location of the MF center. For a left-handed twisted phase, the relation between the axes of DF and LF is

$$\begin{aligned}
\mathbf{x}^{DF} &= \mathbf{x}^{LF}\cos(qz) + \mathbf{y}^{LF}\sin(qz)\\
\mathbf{y}^{DF} &= -\mathbf{x}^{LF}\sin(qz) + \mathbf{y}^{LF}\cos(qz)\\
\mathbf{z}^{DF} &= \mathbf{z}^{LF} = \mathbf{u}_{hx}
\end{aligned} \tag{2}$$

where $q = 2\pi/p$ is a wavevector's modulus being p the pitch of the phase. With reference to the DF axes, the new stochastic variables are $(\mathbf{r}^{DF},\Omega') = Q'$ and the distribution function is invariant under molecular translation, i.e., $p_{eq}(Q') \equiv p_{eq}(\Omega')$. Such a change of variables has been exploited in order to derive the expression of the diffusion coefficient for macroscopic translation monitored along a generic direction $\mathbf{u}$ in a left-handed cholesteric; see part I for the formal derivation starting from the definition eq (1).

As a representative case, in this work we consider the diffusion along the direction of the helical axis of the phase, $\mathbf{u}_{hx}$. By employing the same notation introduced in I, and specifying the general expressions for $\mathbf{u} \equiv \mathbf{u}_{hx}$, the diffusion coefficient $D_{mt}(\mathbf{u}_{hx})$ results as

$$D_{mt}(\mathbf{u}_{hx}) = \overline{\mathbf{u}_{hx}\cdot\mathbf{D}^{DF}_{TT}(\Omega')\mathbf{u}_{hx}} - \int d\Omega' f(\Omega')(\Gamma'_0)^{-1} f(\Omega') p_{eq}(\Omega') \tag{3}$$

with the function $f(\Omega')$ given by

$$f(\Omega') = p_{eq}(\Omega')^{-1}\mathbf{u}_{hx}\cdot\mathbf{D}^{DF}_{TR}(\Omega')\mathbf{M}^{DF}p_{eq}(\Omega') + q\,\mathbf{u}_{hx}\cdot\mathbf{D}^{DF}_{TT}(\Omega')\mathbf{u}_{hx}p_{eq}(\Omega')^{-1}M^{DF}_z p_{eq}(\Omega') \tag{4}$$

and the following operator Γ_0' acting on the orientational degrees of freedom

$$\Gamma_0' = -\begin{pmatrix} q\,\mathbf{u}_{hx} M_z^{DF} \\ \mathbf{M}^{DF} \end{pmatrix} \cdot \mathbf{D}^{DF}(\Omega') p_{eq}(\Omega') \begin{pmatrix} q\,\mathbf{u}_{hx} M_z^{DF} \\ \mathbf{M}^{DF} \end{pmatrix} p_{eq}(\Omega')^{-1} \tag{5}$$

where $\mathbf{M}^{DF}$ is the infinitesimal rotation operator expressed in the DF. In the equations above, $\mathbf{D}^{DF}(\Omega')$ is the 6×6 diffusion matrix for the RT small-steps dynamics referred to the DF axes, which is partitioned into pure translational (TT), pure rotational (RR), and coupling roto-translational (RT, TR) 3×3 blocks.

It should be stressed that eqs (3)-(5) have been derived by exploiting the symmetry relations for the blocks of $\mathbf{D}^{DF}(\Omega')$ holding if the origin of MF is chosen coincident with the Center of Diffusion, as anticipated. According to such a choice, the off-diagonal blocks result symmetric and therefore identical. In fact, $\mathbf{D}^{DF}(\Omega')$ can be related to the (constant) diffusion matrix referred to the MF axes, $\mathbf{D}^{MF}$, by means of the following transformation under rotation of the reference frame,

$$\mathbf{D}^{DF}(\Omega') = (\mathbf{E} \oplus \mathbf{E}) \mathbf{D}^{MF} (\mathbf{E} \oplus \mathbf{E})^{tr} \tag{6}$$

where $\mathbf{E}(\Omega')$ is the Euler matrix related to the MF$\rightarrow$DF transformation. If the origin of MF is placed in CD, then $\mathbf{D}_{TR}^{MF} = (\mathbf{D}_{RT}^{MF})^{tr} = \mathbf{D}_{RT}^{MF}$ and the same relations hold also for the blocks of $\mathbf{D}^{DF}(\Omega')$ through eq (6). Thus, employment of equations (3)-(5) only requires to locate the origin of MF at the CD point, while no restrictions about the orientation of the MF axes are imposed.

The diffusion matrix referred to MF can be evaluated on the basis of generalized Stokes equations for RT motion of the molecule treated as a macroscopic-like object embedded in isotropic viscous environment. The connection between frictional force/torque ($\mathbf{F}$ and $\mathbf{N}$) and linear/angular velocities of the body ($\mathbf{v}$ and $\boldsymbol{\omega}$) is realized through the viscous tensor, $\boldsymbol{\xi}^{MF}$, partitioned into translational, rotational and coupling blocks,

$$\begin{pmatrix} \mathbf{F} \\ \mathbf{N} \end{pmatrix} = -\boldsymbol{\xi}^{MF} \begin{pmatrix} \mathbf{v} \\ \boldsymbol{\omega} \end{pmatrix} = -\begin{pmatrix} \boldsymbol{\xi}_{TT}^{MF} & \boldsymbol{\xi}_{TR}^{MF} \\ \boldsymbol{\xi}_{RT}^{MF} & \boldsymbol{\xi}_{RR}^{MF} \end{pmatrix} \begin{pmatrix} \mathbf{v} \\ \boldsymbol{\omega} \end{pmatrix} \tag{7}$$

Evaluation of $\boldsymbol{\xi}^{MF}$ requires the solution of the hydrodynamical problem for the specific body under consideration [4, 5, 6, 9, 10]. Once $\boldsymbol{\xi}^{MF}$ is specified, Einstein's relation allows

the evaluation of the diffusion matrix in the molecular frame as

$$\mathbf{D}^{MF} = k_B T (\boldsymbol{\xi}^{MF})^{-1} \tag{8}$$

Further input in eqs (3)-(5) is the equilibrium distribution, which can be specified by means of the orientational potential $V_q(\Omega')$ acting on the molecule and quantifying the degree of alignment of the molecular axes with respect to DF. The corresponding Maxwell-Boltzmann distribution is specified as

$$p_{eq}(\Omega') = \frac{e^{-V_q(\Omega')/k_B T}}{\int d\Omega' e^{-V_q(\Omega')/k_B T}} \tag{9}$$

The dependence of the orientational potential on the pitch is explicitly indicated by the subscript "q" (we omit such a subscript for the equilibrium distribution). Such a dependence is due to the twist of the phase as sensed at the molecular level [15]. Intuitively, the main pitch-dependent effects on the molecular alignment are i) a modulation of the strength of orientational ordering with respect to the local director (the $\mathbf{x}^{DF}$ axis), and ii) the appearance of phase biaxiality about such an axis [15]. To quantify these effects we introduce a more natural director frame, DF'$= (\mathbf{x}^{DF'}, \mathbf{y}^{DF'}, \mathbf{z}^{DF'})$, with $\mathbf{z}^{DF'}$ taken along the local director and $\mathbf{x}^{DF'}$ collinear to the helical axis. With respect to DF', the molecular orientation is denoted by Ω''. By adopting the same choice made in ref. [12], we quantify the molcular alignment in DF' by means of the following set of second-rank order parameters,

$$\begin{aligned}
\langle R^2_{0,0} \rangle_{\mathrm{DF'}} &\equiv \overline{D^2_{0,0}(\Omega'')} \\
\langle R^2_{2,0} \rangle_{\mathrm{DF'}} &\equiv \mathrm{Re}\left\{ \overline{D^2_{2,0}(\Omega'')} \right\} \\
\langle R^2_{0,2} \rangle_{\mathrm{DF'}} &\equiv \mathrm{Re}\left\{ \overline{D^2_{0,2}(\Omega'')} \right\} \\
\langle R^2_{2,2} \rangle_{\mathrm{DF'}} &\equiv \frac{1}{2}\mathrm{Re}\left\{ \overline{D^2_{2,2}(\Omega'')} + \overline{D^2_{2,-2}(\Omega'')} \right\}
\end{aligned} \tag{10}$$

where $D^J_{m,k}(\Omega'')$ are rotational Wigner functions [11] and the averages are performed with respect to the equilibrium distribution. Notice that $\langle R^2_{0,0} \rangle_{\mathrm{DF'}}$ is the common second-rank order parameter $\overline{P_2}$ which quantifies the degree of alignment of the molecular axis $\mathbf{z}^{MF}$ with respect to the local director (at the origin of MF); the parameter $\langle R^2_{2,0} \rangle_{\mathrm{DF'}}$ quantifies the degree of phase biaxiality about the director (it vanishes for uniaxial nematic alignment),

$\langle R^2_{0,2}\rangle_{\mathrm{DF}'}$ specifies the molecular biaxiality about $\mathbf{z}^{MF}$, and finally $\langle R^2_{2,2}\rangle_{\mathrm{DF}'}$ reflects the global biaxiality of phase and molecule [12] .

In summary, the required *physical ingredients* to be specified are: i) the pitch of the phase, ii) the (pitch-dependent) orientational potential acting on the probe molecule and referred to the DF axes, $V_q(\Omega')$, and iii) the roto-translational friction tensor referred to the MF axes, $\boldsymbol{\xi}^{MF}$. Once these ingredients are supplied, the numerical estimation of $D_{mt}(\mathbf{u}_{hx})$ is achieved by solving eqs (3)- (5). In the next section we outline the computational methodology employed to solve the leading equations for a given parameterization of the system.

3 Computational methodology

In this section we describe the routes to parameterize the problem, and the procedure for the numerical evaluation of $D_{mt}(\mathbf{u}_{hx})$ according to eqs (3)-(5). Technical details are supplied as Supporting Information [8].

At the implementation stage, the orientational potential $V_q(\Omega')$ and the elements of $\mathbf{D}^{DF}(\Omega')$ are conveniently expanded on the base of Wigner rotational functions [11]. By exploiting the relation $\mathbf{M}^{DF} = i\mathbf{J}^{DF}$, where $\mathbf{J}^{DF}$ is the angular momentum operator with components referred to the DF axes, the action of the rotation operator on the Wigner functions can be easily explicitated (see the Supporting Information [8]). Therefore, (normalized) Wigner functions constitute the elements of the natural orthonormal base onto which the integral eq (3) can be expanded. Along this line, first we introduce the parameterization of the orientational potential acting on the single molecule, then we give the explicit form of the angular dependence of the diffusion matrix elements referred to the DF axes. Finally, the tools for the numerical solution of the problem are outlined.

3.1 The orientational potential

The derivation of the q-dependent orientational potential acting on a generic molecule in the twisted director field is treated in detail in ref. [15]. The construction of the potential is based on the phenomenological "surface interactions model" [13]. In such a model one assumes that the net molecular alignment results from contributions of all elements of the exposed molecular surface: each surface element at a point P is forced to "contain" the local director experienced at such location, through a second-rank interaction which destabilizes the alignment of the surface-normal along the director itself; then, the overall mean-field potential acting on the molecule at orientation Ω' is given by the following surface integral

$$\frac{V_q(\Omega')}{k_B T} = \epsilon \int_S d\sigma(P)\, P_2(\mathbf{s}(P,\Omega') \cdot \mathbf{n}(P,\Omega')) \tag{11}$$

where $\mathbf{s}(P,\Omega')$ is the normal vector to the surface (with Cartesian components referred to DF) at the point P, $\mathbf{n}(P,\Omega')$ is the director experienced at the same location, and $P_2(\cdots)$ is the second-rank Legendre polynomial. The parameter $\epsilon > 0$ (having physical units of inverse surface area) quantifies the strength of the alignment.

In ref. [15], the general form eq (11) is elaborated for the specific case of helical director field probed at the molecular length-scale. The analysis leads to the following general expansion on the base of rotational Wigner functions

$$\frac{V_q(\Omega')}{k_B T} = \sum_{m=0,\pm 2} \sum_{k=-2}^{+2} w_{2,m,k}(q) D^2_{m,k}(\Omega') \; + \sum_{J\geq 3} \sum_{m=\pm 2} \sum_{k=-J}^{+J} w_{J,m,k}(q) D^J_{m,k}(\Omega') \tag{12}$$

where the q-dependent weights $w_{J,m,k}(q)$ can generally be complex-valued, with the constraint $w_{J,m,k}(q)^* = (-1)^{m+k} w_{J,-m,-k}(q)$ imposed by the requirement that the expansion eq (12) must be a real function. These coefficients are related to the molecular symmetry, dimensions and surface topology.

As the pitch increases with respect to the linear dimensions of the molecule, the second-rank terms for $J = 2$ become dominant in eq (12). In the present work we refer to such a limit case by adopting the following model form for the potential

$$\frac{V_q(\Omega')}{k_B T} = \sum_{m,k=-2}^{+2} w_{2,m,k}(q) D^2_{m,k}(\Omega') \tag{13}$$

which is *exact* only for $q = 0$, i.e., for untwisted nematics. The explicit form of the coefficients $w_{2,m,k}(q)$ will be reported for the case of ellipsoidal molecule (see section 5). These coefficients constitute the input parameters about the *statics* of the system. We stress that, even at this lowest level of approximation, the main effects of the director twist discussed in section 2 can be captured.

3.2 Orientational dependence of the diffusion matrix referred to DF

The orientational dependence of the diffusion matrix referred to the DF system of axes is fully specified by eq (6). However, we need an operative form of such dependence in terms of Wigner rotational functions rather than products of Euler matrix elements. This can be achieved first by exploiting the transformation properties of the irriducible spherical components of the second-rank tensorial blocks $\mathbf{D}^{DF}_{TT}$, $\mathbf{D}^{DF}_{RR}$, $\mathbf{D}^{DF}_{RT} \equiv \mathbf{D}^{DF}_{TR}$ under rotation of the reference frame [11], and then converting back to Cartesian components (see the Supporting Information [8]). The resulting expression is

$$\left[D^{DF}_{**}(\Omega')\right]_{ij} = \sum_{L=0,2} \sum_{M,M'=-L}^{+L} \gamma^{**}_{ij}(L, M, M') D^{L}_{M,M'}(\Omega')^{*} \tag{14}$$

where $**$ stands for TT, RR, RT≡TR, and the indices i, j label the axes of DF. The sum eq (14) is restricted to $L = 0, 2$ because all the blocks are second-rank symmetric tensors. The coefficients $\gamma^{**}_{ij}(L, M, M')$ result as combinations of elements of $\mathbf{D}^{MF}$, and are explicitly given in the Supporting Information [8]. Thus, the elements of the matrix $\mathbf{D}^{MF}$ constitute the input parameters for the *dissipative dynamics*, and can be evaluated from eq (8) once the friction tensor is supplied.

3.3 The matrix handling

Hereafter we outline the procedure adopted to calculate $D_{mt}(\mathbf{u}_{hx})$ according to eqs (3)-(5). The first addendum at the r.h.s. of eq (3) is simply an equilibrium average which can be evaluated by employing the expansion eq (14) for the specific element of the TT block (the explicit expression is given in the Supporting Information [8]). From now on we focus on

the route to evaluate the second addendum of eq (3). Apart of the sign, such a contribution can be rewritten as

$$\int d\Omega' \, f(\Omega') \, (\Gamma'_0)^{-1} f(\Omega') p_{eq}(\Omega') \equiv \int_0^\infty dt \, G(t) \tag{15}$$

with

$$G(t) = \int d\Omega' \, f(\Omega') e^{-\Gamma'_0 t} f(\Omega') p_{eq}(\Omega') \tag{16}$$

One can recognize that $G(t)$ has the same structure of the integral specifying a rotational time-correlation function, and that the r.h.s. of eq (15) is nothing but its spectral density (Fourier-Laplace transform) evaluated at zero-frequency. Such interpretation of the second addendum of eq (3) avoids to work with the inverted operator $(\Gamma'_0)^{-1}$, and allows one to adopt the standard methodologies used for the calculation of time-correlation functions.

First we employ the symmetrized form of the evolution operator, $\tilde{\Gamma}'_0 = p_{eq}^{-1/2}(\Omega') \Gamma'_0 p_{eq}^{1/2}(\Omega')$, so converting eq (16) into the following symmetric form

$$G(t) = \int d\Omega' \, f(\Omega') p_{eq}^{1/2}(\Omega') e^{-\tilde{\Gamma}'_0 t} f(\Omega') p_{eq}^{1/2}(\Omega') \equiv \langle F(\Omega')^* | e^{-\tilde{\Gamma}'_0 t} | F(\Omega') \rangle \tag{17}$$

with $F(\Omega') = f(\Omega') p_{eq}(\Omega')$. For the latter identity in eq (17), the conventional bra-ket notation has been adopted to represent the hermitian scalar product with general properties

$$\begin{aligned} \langle f_1(\Omega') | f_2(\Omega') \rangle &\equiv \int d\Omega' \, f_1(\Omega')^* f_2(\Omega') = \langle f_2(\Omega') | f_1(\Omega') \rangle^* \\ \langle f_1(\Omega') | \mathcal{O} | f_2(\Omega') \rangle &\equiv \int d\Omega' \, f_1(\Omega')^* \mathcal{O} f_2(\Omega') = \langle f_2(\Omega') | \mathcal{O}^\dagger | f_1(\Omega') \rangle^* \end{aligned} \tag{18}$$

being $\mathcal{O}$ is a generic operator acting on functions of Ω', and $\mathcal{O}^\dagger$ denoting its adjoint.

Equation (17) can be expanded onto a complete set of orthonormal functions spanning the space of the Euler angles, yielding a matrix form of the scalar product. As mentioned before, the natural choice is that of using the normalized Wigner functions

$$|N\rangle \equiv |j_N, m_N, k_N\rangle = \left(\frac{2j_N + 1}{8\pi^2} \right)^{1/2} D^{j_N}_{m_N, k_N}(\Omega') \quad , \quad \langle N | N' \rangle = \delta_{N,N'} \tag{19}$$

with $N \equiv (j_N, m_N, k_N)$ denoting the cumulative set of indices of the basis elements of ranks $j_N \geq 0$ and $m_M, k_M = -J_N, \cdots, +J_N$. In practic, a finite-size matrix is handled

by truncating the rank j_N in correspondence of a given value j_{max}. Equation (17) is thus converted into

$$G(t) = \mathbf{F}^{Tr} e^{-\tilde{\mathbf{\Gamma}}'_{\mathbf{0}} t} \mathbf{F} \tag{20}$$

with the elements of the vector $\mathbf{F}$ and of the complex-hermitian matrix $\tilde{\mathbf{\Gamma}}'_{\mathbf{0}}$ given by

$$(\mathbf{F})_N = \langle N|F(\Omega')\rangle \quad , \quad (\tilde{\mathbf{\Gamma}}'_{\mathbf{0}})_{N_1,N_2} = \langle N_1|\tilde{\Gamma}'_0|N_2\rangle \tag{21}$$

and to be formally evaluated according to eqs (18). The explicit form of $\tilde{\Gamma}'_0$ can be derived from the symmetrization of Γ'_0 given in eq (5). By employing $\mathbf{M}^{DF} = i\mathbf{J}^{DF}$, and considering the equivalence of the TR and RT blocks of the diffusion matrix, one gets

$$\begin{aligned}\tilde{\Gamma}'_0 = q^2\, \mathcal{O}_z^\dagger \mathbf{u}_{hx} \cdot \mathbf{D}^{DF}_{TT}(\Omega')\mathbf{u}_{hx}\mathcal{O}_z + q\, \left[\mathcal{O}_z^\dagger \mathbf{u}_{hx} \cdot \mathbf{D}^{DF}_{RT}(\Omega')\boldsymbol{\mathcal{O}} \,+\, \boldsymbol{\mathcal{O}}^\dagger \mathbf{D}^{DF}_{RT}(\Omega')\mathbf{u}_{hx}\mathcal{O}_z\right] + \\ + \boldsymbol{\mathcal{O}}^\dagger \mathbf{D}^{DF}_{RR}(\Omega')\boldsymbol{\mathcal{O}}\end{aligned} \tag{22}$$

with the following (not hermitean) vectorial operator

$$\boldsymbol{\mathcal{O}} = \frac{1}{2}[\mathbf{J}^{DF} V_q(\Omega')] \,+\, \mathbf{J}^{DF} \tag{23}$$

By employing the expansion of $V_q(\Omega')$ on the base of Wigner functions, the integrals for the matrix elements in eq (21) can be subdivided into terms of the kind

$$\langle N_1|\mathcal{O}_\alpha^\dagger g_{\alpha\beta}(\Omega')\mathcal{O}_\beta|N_2\rangle \tag{24}$$

where the functions $g_{\alpha\beta}(\Omega')$ assume specific forms according to the different contributions in eq (22). Integration by parts allows the convertion of eq (24) into the form

$$\langle(\mathcal{O}_\alpha \Phi_{N_1}(\Omega'))|g_{\alpha\beta}(\Omega')(\mathcal{O}_\beta \Phi_{N_2}(\Omega')\rangle \tag{25}$$

with $\Phi_N(\Omega') \equiv |N\rangle$ given in eq (19). Therefore, one needs to specify the action of the components of $\boldsymbol{\mathcal{O}}$ on the bra- and -ket functions, and then to evaluate the integral eq (25).

Evaluation of these integrals requires the reiterated use of standard tools of the angular momentum algebra [11], and in particular: (i) explicit action of the J^{DF}_α components on the Wigner functions; (ii) exploitation of the symmetry properties of the Wigner functions $D^j_{m,k}(\Omega')$ and of the coefficients $w_{2,m,k}(q)$ in eq (13) under change of sign of the projection

indeces m, k; (iii) explicit integration of products of several Wigner functions (up to 5) involving the Clebsch-Gordan coupling coefficients [11]; (iv) compact keeping of the expressions. Since the algebra is quite elaborated, for the benefict of future applications the resulting expressions of the matrix elements $(\tilde{\mathbf{\Gamma}}'_{\mathbf{0}})_{N_1,N_2}$, of the vector elements $(\mathbf{F})_N$, and of the first addendum in eq (3) are supplied in the Supporting Information [8]. Even if the procedure above outlined is quite general, the explicit relations refer to the case of $V_q(\Omega')$ approximated to second order terms as in eq (13).

The scalar product eq (20) can be then evaluated by recurring to the Lanczos algorithm [16] for the complex-hermitian matrix $\tilde{\mathbf{\Gamma}}'_{\mathbf{0}}$. The Lanczos procedure generates the optimal subspace of functions onto which such scalar product can be expanded. Such a subspace consists of a bi-orthonormal base of functions divided into *left* (L) and *right* (R) subgroups, whose elements are denoted respectively by $|N_L\rangle$ and $|N_R\rangle$, and with $\langle N_L|N'_R\rangle = \delta_{N,N'}$. This subspace is generated by means of a three-terms iterative procedure involving the elements of $\tilde{\mathbf{\Gamma}}'_{\mathbf{0}}$ and starting from the first elements $|1_L\rangle = |F(\Omega')^*\rangle/\mathcal{N}$ and $|1_R\rangle = |F(\Omega')\rangle/\mathcal{N}$, where $\mathcal{N}^2 = \langle F(\Omega')^2\rangle$ ensures the normalization $\langle 1_L|1_R\rangle = 1$. The vectorial representation of these functions are the so-called *left-* and *right- starting vectors*, whose elements are respectively $\langle N|1_L\rangle = (\mathbf{F})^*_N/\mathcal{N}$ and $\langle N|1_R\rangle = (\mathbf{F})_N/\mathcal{N}$. The dimension of the generated subspaces equals the chosen number of iterations (nsteps). Equation (20) is then converted into

$$G(t) = \mathcal{N}^2\langle 1_L|e^{-\tilde{\Gamma}'_0 t}|1_R\rangle = \mathcal{N}^2\left[e^{-\mathbf{T}t}\right]_{1,1} \tag{26}$$

where $\mathbf{T}$ is the tri-diagonal matrix

$$i,j = 1,\cdots,\text{nsteps}: \qquad (\mathbf{T})_{i,j} = \alpha_i\delta_{i,j} + \beta_{\min\{i,j\}+1}\,\delta_{|i-j|,1} \tag{27}$$

with α_i, β_i (generally complex) generated by the iterative procedure. Then, by inserting eq (26) into eq (15), the required spectral density at zero-frequency results as $\mathcal{N}^2[\mathbf{T}^{-1}]_{1,1}$. By exploiting the basic block-partitioning of the inverse matrix to evaluate the element $1,1$ one gets the following continued-fraction form

$$\int_0^\infty dt G(t) = \mathcal{N}^2\left[\mathbf{T}^{-1}\right]_{1,1} = \cfrac{\mathcal{N}^2}{\alpha_1 - \cfrac{\beta_2^2}{\alpha_2 - \cfrac{\beta_3^2}{\alpha_3 - \cdots}}} \tag{28}$$

which is (apart of the sign) the second addendum at the r.h.s of eq (3).

At the computational stage, FORTRAN codes have been written to implement the methodology above described. The check of the convergence on the values of $D_{mt}(\mathbf{u}_{hx})$ has been done with respect to the extension of the orthonormal base (i.e., with respect to j_{max}), and to the number of steps of the Lanczos procedure (nsteps). In all the cases presented in this work, convergence within $5 \times 10^{-3}\%$ has been achieved with $j_{max} = 8$ and nsteps $= 200$. It should be stressed that the Lanczos procedure is efficient only in case of sparse matrices $\tilde{\mathbf{\Gamma}}'_{\mathbf{0}}$. On the contrary, from eq (20) one should proceede through the time-consuming direct inversion of the (generally very large) matrix $\tilde{\mathbf{\Gamma}}'_{\mathbf{0}}$, or equivalent procedures like the diagonalization route. Notice that the use of an orientational potential containing only second-rank terms (see eq (13)) allows one to keep the matrix $\tilde{\mathbf{\Gamma}}'_{\mathbf{0}}$ sufficiently sparse.

4 Archetype molecules and outlines of model calculations

For the model calculations of $D_{mt}(\mathbf{u}_{hx})$ versus the pitch of the twisted phase we chose three archetype molecules: 1) an ellipsoidal molecule with no RT coupling in the roto-translational diffusion matrix, 2) a bent-rod molecule having RT coupling, and 3) a chiral propeller-like molecule made of two twisted disks. The analysis will start from the simplest archetype geometry, i.e., the ellipsoidal molecule. The purpose is to evaluate, separately, the effects on $D_{mt}(\mathbf{u}_{hx})$ due to: i) the phase biaxiality induced by the director twist at the molecular length-scale; ii) the increasing of the local order parameter $\overline{P_2} = \langle R^2_{0,0} \rangle_{DF'}$; iii) the slowdown of the rotational dynamics about the molecular short-molecular axes. Then we will turn to biaxial molecules possessing RT coupling in the microscopic diffusion matrix, beginning with the bent-rod molecule; consideration of the two geometric enantiomers of the propeller-like molecule will complete the analysis by exploring the effects of the shape's chirality feature.

As previously discussed, inputs for the calculation are the diffusion matrix in the molecular frame, obtained by inverting the friction tensor $\boldsymbol{\xi}^{MF}$ according to Einstein's relation eq (8), and the (pitch-dependent) coefficients $w_{2,m,k}(q)$ entering eq (13) for the orientational po-

tential. These quantities are specified for the three archetype geometries in the next sections; the following remarks should highlight the general approach to the parameterization.

To evaluate the elements of $\boldsymbol{\xi}^{MF}$ we invoke standard models for the RT friction of a rigid body moving in an isotropic fluid [4, 5, 6, 9, 10]. These approaches are based on the solution of the quasi-static form of the hydrodynamic equations for creeping motion of the fluid, which requires to confine the analysis to small values of both the translational and the rotational Reynolds numbers [5]. The fluid is treated as incompressible, and inertial contributions are neglected with respect to the viscous terms in the Navier-Stokes equation. The simplified equations of the motion are solved by imposing the fluid to be at rest at infinite distance from the body, and by using stick boundary conditions of the velocity field at the body's surface. In despite of these unrealistic boundary conditions if applied to objects of molecular dimensions, these models provide friction coefficients that allow an accurate reproduction of spectroscopic observables sensitive to the RT motions of single molecules in the overdamped regime. Nevertheless, we want to stress that these models approximate the molecular environment to an (average) isotropic fluid with (average) shear viscosity η. Therefore, the assumption we are forced to make is that the nematic-like environment is probed by the molecule as an isotropic medium from the point of view of the viscous drag. Identification of the *effective* viscosity η from the dissipative coefficients entering the stress tensor for the locally anisotropic phase (which are, at least, the five independent Leslie coefficients for uniaxial nematic alignment [2]) is not a trivial task. On the other hand, the viscosity enters only as a scaling parameter for $D_{mt}(\mathbf{u}_{hx})$. Since we are interested in *relative* variations of the transport coefficient versus the pitch of the phase, an accurate estimation of η is not required; the value $\eta = 0.01$ Pa s, which is within the typical range of shear viscosities of low molecular-weight nematics [2], will be used in all the calculations referred to $T = 300$ K.

Concerning the parameterization of the orientational potential, we take into account that the local biaxiality due to the director twist at the molecular length-scale is very small even for short pitches [15]. Our hypothesis is that the biaxiality would introduce only a minor correction to the values of $D_{mt}(\mathbf{u}_{hx})$ evaluated for uniaxial alignment. Accordingly,

the parameterization of the orientational potential at $q = 0$ constitutes the reference for all archetype molecules. In order to validate such assumption, the correction due to the local biaxiality will be quantified only for the simplest object, i.e., the ellipsoidal molecule.

Finally, the larger linear dimension of 30 Å is chosen for the archetype molecules. In all the cases, calculations of $D_{mt}(\mathbf{u}_{hx})$ have been done for several values of the pitch ranging from 500 Å up to very long pitches corresponding to the untwisted nematic phase.

5 Ellipsoidal molecule

Let us consider an ellipsoid of revolution about its major axis, i.e., a prolate spheroid of lentgh $2a$ and width $2b$ with $a > b$. The axis $\mathbf{z}^{MF}$ of MF is taken along the major axis of the ellipsoid, while the transverse axes are arbitrarily chosen due to the cylindric symmetry of the molecule (see Fig. 2). Due to the molecular symmetry, the origin of MF (the Center of Diffusion) coincides with the center of mass. No roto-translational coupling emerges in the friction matrix, i.e., $\boldsymbol{\xi}^{MF}_{RT} = \boldsymbol{\xi}^{MF}_{TR} = 0$. Moreover the diagonal blocks of the friction matrix, $\boldsymbol{\xi}^{MF}_{TT}$ and $\boldsymbol{\xi}^{MF}_{RR}$, are uniaxial tensors both diagonal in the adopted MF.

The elements of the friction matrix are quantified by means of Perrin's model based on the solution of the hydrodynamic equations employing stick-boundary conditions at the molecular surface [5]. The leading expressions are hereafter summarized. For the translational block one has

$$\begin{aligned}
\left(\xi^{MF}_{TT}\right)_{XX} &= \left(\xi^{MF}_{TT}\right)_{YY} = 32\pi \frac{a^2 - b^2}{(2a^2 - 3b^2)S + 2a}\eta \\
\left(\xi^{MF}_{TT}\right)_{ZZ} &= 16\pi \frac{a^2 - b^2}{(2a^2 - b^2)S - 2a}\eta
\end{aligned} \tag{29}$$

while for the rotational block

$$\begin{aligned}
\left(\xi^{MF}_{RR}\right)_{XX} &= \left(\xi^{MF}_{RR}\right)_{YY} = \frac{32\pi}{3} \frac{a^4 - b^4}{(2a^2 - b^2)S - 2a}\eta \\
\left(\xi^{MF}_{RR}\right)_{ZZ} &= \frac{32\pi}{3} \frac{(a^2 - b^2)b^2}{2a - b^2 S}\eta
\end{aligned} \tag{30}$$

where the quantity S is defined as

$$a > b: \qquad S = \frac{2}{\sqrt{a^2 - b^2}} \ln \frac{a + \sqrt{a^2 - b^2}}{b} \tag{31}$$

and η is the viscosity of the molecular environment. Then, the required non-vanishing elements of the diffusion matrix are given by

$$i = X, Y, Z: \qquad \left(D_{TT}^{MF}\right)_{ii} = k_B T \left(\xi_{TT}^{MF}\right)_{ii}^{-1} \quad , \quad \left(D_{RR}^{MF}\right)_{ii} = k_B T \left(\xi_{RR}^{MF}\right)_{ii}^{-1} \tag{32}$$

The diffusion matrix has been evaluated for the geometrical parameters indicated in Fig. 2, and for $\eta = 0.01$ Pa s, $T = 300$ K. The values are reported in Table 1.

We turn now to specify the alignment properties of the molecule. In order to parameterize the pitch-dependent orientational potential, we adopt the surface interaction model (see section 2) in the form developed in ref. [15]. The modeling requires the parameterization of the ellispoidal surface by employing spherical coordinates referred to the MF axes, i.e., θ and ϕ as polar and azimuthal angles identifying a surface point at distance $r_0(\theta)$ from the origin of MF. For the specific geometry, the orientational potential results to be expressed as

$$\frac{V_q(\Omega')}{k_B T} = \sum_{m=0,\pm 2} w_{2,m,0}(q) D_{m,0}^2(\Omega') \; + \sum_{J \geq 4,\, \text{even}} \sum_{m=\pm 2} w_{J,m,0}(q) D_{m,0}^J(\Omega') \tag{33}$$

with the coefficients of the expansion given by

$$w_{J,m,0}(q) = \epsilon \, d_{m,0}^2(\pi/2) \sum_{l=|J-2|,\, \text{even}}^{J+2} \sum_{n=-l}^{+l} (-1)^{l/2} \, I_{l,n,m,-n}(q) \, C(l,2,J;0,m) C(l,2,J;n,-n) \tag{34}$$

where $C(J_1, J_2, J_3; m_1, m_2)$ are Clebsch-Gordan coefficients and $d_{l,m}^J(\cdots)$ are *reduced* Wigner functions [11]. The factors $I_{l,n,m,-n}(q)$ are the following q-dependent molecular-surface integrals

$$I_{l,n,m,-n}(q) = 2\pi(2l+1) \int_0^\pi d\theta \sin\theta \sqrt{r_0(\theta)^4 + (a^2 - b^2)^2 \sin^2\theta \cos^2\theta} \times \\ \times j_l(|m| q r_0(\theta)) \; d_{n,0}^l(\theta) \; \chi_n(\theta) \tag{35}$$

with $r_0(\theta) = [a^2 - (a^2 - b^2)\sin^2\theta]^{1/2}$, and the functions $\chi_n(\theta)$ defined as

$$\chi_n(\theta) = \begin{cases} d_{-n,0}^2(\theta + \beta(\theta)) & \text{if } 0 \leq \theta \leq \pi/2 \\ d_{-n,0}^2(\theta - \beta(\theta)) & \text{if } \pi/2 < \theta \leq \pi \end{cases} \tag{36}$$

for $a > b$, where

$$\beta(\theta) = \arccos\left[1 + \left(\frac{(a^2 - b^2)\sin\theta\cos\theta}{a^2 - (a^2 - b^2)\sin^2\theta}\right)^2\right]^{-1/2} \tag{37}$$

In eq (35) $j_l(\cdots)$ are spherical Bessel functions of rank l [14]. The weights $w_{J,m,0}(q)$ can be determined for each q value once the strength-parameter ϵ is specified. Values of ϵ have been tuned in order to yield $\overline{P_2} \simeq 0.60$ and $\overline{P_2} \simeq 0.80$ in the infinite-pitch limit (uniaxial alignment), and then used to parameterize the potential at finite pitch values. The employed values, together with the generated order parameters referred to the DF' axes (see eqs (10)), are reported in Table 1.

In Fig. 5 we show the calculated profile of $D_{mt}(\mathbf{u}_{hx})$ versus the pitch for $\overline{P_2} \simeq 0.60$. The full circles are referred to calculations performed without accounting for the biaxiality of the phase induced by the director twist, while the open circles are referred to calculations including such a dependence on the orientational potential. First we note that both profiles tend to a limit value as the pitch increases, $D_{mt}(\mathbf{u}_{hx})_\infty$; such a value corresponds to the diffusion of the probe in the (untwisted) nematic phase along an arbitrary direction perpendicular to the macroscopic director. By looking at the same profiles in the other way round, the twist of the phase causes a slowdown of the macroscopic migration along the helical pitch. Notice that the variations of $D_{mt}(\mathbf{u}_{hx})$ with respect to $D_{mt}(\mathbf{u}_{hx})_\infty$ are very small. For the profile with full circles, the largest variation referred to the asymptotic value is less than 1.5%.

The inclusion of the phase biaxiality induced by the twist of the director field produces a further slowdown of the translational diffusion, but the contribution to the value of $D_{mt}(\mathbf{u}_{hx})$ is roughtly only 1/10 of the total amount. Therefore, at first instance, the local biaxiality of the ordering can be ignored.

We turn now to consider the effect of the increase of the order parameter. In Fig. 6 we compare the profiles for $\overline{P_2} \simeq 0.60$ (open squares) and $\overline{P_2} \simeq 0.80$ (open circles). The calculations have been performed by neglecting the pitch-dependence on the orientational potential, with the purpose to highlight the effect of the order parameter alone. To compare the two profiles, the values of $D_{mt}(\mathbf{u}_{hx})$ are scaled with respect to their (different) asymptotic values at infinite pitch. One sees that the increase of the orientational order induces a slowdown of the macroscopic diffusion. Intuitively, such a slowdown of the translational

dynamics has a frictional source: as $\overline{P_2}$ increases the molecule tends to oppose to the motion its elongated section, causing an increase of the average friction.

We conclude the analysis of the ellipsoidal molecule by investigating the effects due to the decreasing of the rotational diffusion of the molecule about the short axes. In Fig. 7 the profiles of $D_{mt}(\mathbf{u}_{hx})$ versus the pitch are both calculated for $\overline{P_2} \simeq 0.60$ and neglecting the local biaxiality. The full circles are referred to the diffusion coefficients listed in Table 1 (the profile is the same as in Fig. 5), while open squares are referred to the coefficients $(D_{RR}^{MF})_{XX} = (D_{RR}^{MF})_{YY} = 1.88 \times 10^6\ s^{-1}$, i.e., reduced by a factor 10. It appears that the slowdown of the rotational dynamics about the short molecular axes produces a significant reduction of the macroscopic diffusion coefficient: at the shortest pitch, the decrease from the asymptotic value shifts from $\sim 1.5\%$ to $\sim 12\%$. This effect can be qualitatively explained by recurring again to the pictorial connection between small-steps translations along the helix and corresponding *required* rotations of the molecule about the short axes. In fact (for a fixed order parameter) the charateristic rotational times about the short axes increase as $(D_{RR}^{MF})_{XX} = (D_{RR}^{MF})_{YY}$ are reduced, thus inducing a slowdown of the coupled translational motion.

Summarizing, the following considerations can be outlined from the investigation of the simple ellipsoidal molecule: i) an increasing order parameter $\overline{P_2}$ induces a decrease of the macroscopic diffusion coefficient with respect to the asymptotic value at infinite pitch; ii) a major effect on the macroscopic diffusion coefficient is due to the slowdown of the rotational dynamics about the short molecular axes. This suggests that elongated molecules should diffuse slower than short molecules (at fixed order parameter); iii) the phase biaxiality induced by the director twist can be ignored at the first instance, since it contributes only up to $10 - 15\%$ of the total deviation from the asymptotic value at infinite pitch.

According to the latter item one can parameterize the orientational potential in the approximation of locally uniaxial phase ($q = 0$). Such a choice will be adopted for the more complex geometries considered in the following.

6 Bent-rod molecule

Let us consider a bent-rod molecule made of two linked rods. The MF system and the geometrical details of the object are depicted in Fig. 3. In particular, d denotes the displacement between the Center of Diffusion and the junction of the rods (which is always located along the $\mathbf{x}^{MF}$ axis at positive coordinate). The existence of RT coupling in the friction matrix is expected by imaging to translate the molecule along $\mathbf{z}^{MF}$; such a translation will induce a tumbling about the axis $\mathbf{y}^{MF}$. Equivalently, the translation along $\mathbf{y}^{MF}$ would rotate the molecule about $\mathbf{z}^{MF}$.

The elements of the friction matrix are determined by adopting Wegener's model [4]. Let us denote with $\xi_{\perp}^{T}$, $\xi_{\parallel}^{T}$ and $\xi_{\perp}^{R}$, $\xi_{\parallel}^{R}$ the translational and rotational friction coefficients for the separated rods in the viscous environment (the labels $\perp$ and $\parallel$ are referred to the longitudinal and transverse axes of the rods). In the long-rod limit, corresponding to the condition $l/R \gg 1$, the following relations hold [4]

$$\xi_{\perp}^{T} = 2\xi_{\parallel}^{T} = bl \quad , \quad \xi_{\perp}^{R} = bl^3/12 \quad , \quad \xi_{\parallel}^{R} = el^3 \tag{38}$$

with

$$b = 4\pi\eta/\ln(l/R) \quad , \quad e = 8\pi\eta(R/l)^2/3 \tag{39}$$

For sake of compact expressions, we define the following parameters

$$\begin{aligned} f_1 &= 2\xi_{\perp}^{T}\sin^2\alpha/2 + 2\xi_{\parallel}^{T}\cos^2\alpha/2 \\ f_2 &= 2\xi_{\perp}^{T}\cos^2\alpha/2 + 2\xi_{\parallel}^{T}\sin^2\alpha/2 \\ f_3 &= \xi_{\perp}^{R} + (l/2)^2\xi_{\perp}^{T} \end{aligned} \tag{40}$$

where $\pi - \alpha$ is the angle formed by the two rods (see Fig. 3). Wegener's expressions are herefater rewritten according to our notation. For the translational diagonal block one has

$$(\xi_{TT}^{MF})_{XX} = f_2 \quad , \quad (\xi_{TT}^{MF})_{YY} = 2\xi_{\perp}^{T} \quad , \quad (\xi_{TT}^{MF})_{ZZ} = f_1 \tag{41}$$

for the rotational diagonal block

$$(\xi_{RR}^{MF})_{XX} = 2f_3\cos^2\alpha/2 + 2\xi_{\parallel}^{R}\sin^2\alpha/2$$

$$(\xi^{MF}_{RR})_{YY} = 2f_3 + d^2 f_1 - 2d\xi^T_\perp l \sin\alpha/2$$
$$(\xi^{MF}_{RR})_{ZZ} = 2f_3 \sin^2\alpha/2 + 2\xi^R_\parallel \cos^2\alpha/2 + 2d^2\xi^T_\perp - 2d\xi^T_\perp l \sin\alpha/2 \qquad (42)$$

while for the coupling blocks the unique non-vanishing elements are

$$(\xi^{MF}_{RT})_{YZ} = (\xi^{MF}_{TR})_{ZY} = \xi^T_\perp l \sin\alpha/2 - d\, f_1$$
$$(\xi^{MF}_{RT})_{ZY} = (\xi^{MF}_{TR})_{YZ} = -\xi^T_\perp l \sin\alpha/2 + 2d\xi^T_\perp \qquad (43)$$

The displacement d is not known a priori, that is, the location of the CD pole has to be determined from the chosen geometrical parameters. To this purpose we start from a rough estimation of d in the very long-rod limit [4],

$$l/R \gg 1: \qquad d \simeq \frac{2l\sin\alpha/2}{4 - \cos^2\alpha/2 \sin^2\alpha/2} \qquad (44)$$

Then the friction-matrix is built for values $d > 0$ ranging around the above estimation, and the diffusion matrix is obtained as $\mathbf{D}^{MF} = k_B T(\boldsymbol{\xi}^{MF})^{-1}$ for each of them up to find the (unique) d value which yields symmetric RT and TR blocks of the diffusion matrix. For the geometrical parameters indicated in Fig. 3, the estimated value is $d = 4.7$Å. By choosing $\eta = 0.01$ Pa s and $T = 300$ K, the resulting non-vanishing elements of the diffusion matrix are listed in Table 2.

The orientational potential acting on the molecule is parameterized, as stressed at the end of section 5, by neglecting the local biaxiality induced by the director twist. Thus eq (13) is specified as

$$V_{q=0}(\Omega')/k_B T = \sum_{m=0,\pm2} \sum_{k=-2}^{+2} w_{2,m,k}(0) D^2_{m,k}(\Omega') \qquad (45)$$

To evaluate the coefficients $w_{2,m,k}(0)$ we exploit the additive nature of the orientational potential in the case $q = 0$. Correspondingly, $V_{q=0}(\Omega')$ is obtained by summing up the independent contributions from the two rods in the form

$$w_{2,m,k}(0) = d^2_{m,0}(\pi/2)\, c_0 \, \left[D^2_{k,0}(\Omega^{(1)}) + D^2_{k,0}(\Omega^{(2)})\right] \qquad (46)$$

where $\Omega^{(1)} = (\pi, \alpha/2, 0)$ and $\Omega^{(2)} = (\pi, \pi - \alpha/2, 0)$ are the sets of Euler angles which specify the transformations from MF to local frames with longitudinal axes collinear to the long axes

of the rods. Moreover, $c_0 \equiv c_0^{(1)} = c_0^{(2)} < 0$ is a coefficient which quantifies the strength of calamitic alignment of the long axes of the two equivalent rods with respect to the director. By explicitating the involved Wigner functions, some algebraic rearrangements of eq (46) yield the following expressions of the non-vanishing coefficients for $m = 0, \pm 2$

$$
\begin{aligned}
w_{2,m,0}(0) &= d^2_{m,0}(\pi/2)\, c_0\, (3\cos^2\alpha/2 - 1) \\
w_{2,m,\pm 2}(0) &= d^2_{m,0}(\pi/2)\, c_0\, \sqrt{3/2}\sin^2\alpha/2
\end{aligned}
\tag{47}
$$

The coefficient c_0 is chosen to generate a local order parameter $\overline{P_2} \equiv \langle R^2_{0,0}\rangle_{DF'} \simeq 0.60$. The values of c_0 and of the generated order parameters (see eqs (10)) are collected in Table 2.

Based on the above parameterization, calculations of $D_{mt}(\mathbf{u}_{hx})$ have been done for several values of the pitch; the resulting profile is plotted in Fig. 8. One can see that the profile resembles that of the ellipsoidal molecule, that is no new features emerge when the sole RT coupling is inserted in the diffusion matrix. Even for the bent-rod, an increasing twist of the phase produces a slowdown of the macroscopic diffusion. The largest variation from the asymptotic profile at infinite pitch, evaluated at $p = 500$ Å, is $\sim 0.8\%$, that is of the same order of magnitude of that for the ellispoidal object of comparable dimensions.

7 Propeller-like molecule

We consider now a propeller-like molecule made of two identical disks rigidly linked and tilted one with respect to the other by an angle 2ψ. The adopted molecular frame and the geometrical parameters are shown in Fig. 4. The Center of Diffusion coincides with the middle point along the connecting line. The object possesses shape chirality, with the two enantiomers characterized by opposite signes of the angle ψ. The shape chirality determines RT coupling in the friction (and diffusion) matrix. The presence of RT coupling is intuitive by imaging to translate the object along the axis $\mathbf{x}^{MF}$; such a motion will induce the well known rotation of the propeller about $\mathbf{x}^{MF}$ itself. Also, the translation along $\mathbf{y}^{MF}$ induces rotation about the same axis. The clock- or anticlockwise character of the induced rotations

depends on the sign of the elements of the corresponding RT (TR) block, which is opposite for the two enantiomers.

The elements of the friction matrix are determined by adopting the model of Happel and Brenner [5]. Hereafter we summarize the approximated expressions of the friction tensor elements in MF, which constitute the zero-th order truncation of full expansion into powers of $R/h \ll 1$, where R is the radius of the disks while h denotes the separation of their centres. For the translational block one has

$$\begin{aligned}(\xi^{MF}_{TT})_{XX} &= \frac{32}{3}\eta\, R(2+\cos^2\psi)\\ (\xi^{MF}_{TT})_{YY} &= \frac{32}{3}\eta\, R(2+\sin^2\psi)\\ (\xi^{MF}_{TT})_{ZZ} &= \frac{64}{3}\eta\, R\end{aligned} \tag{48}$$

then for the rotational one

$$\begin{aligned}(\xi^{MF}_{RR})_{XX} &= \frac{32}{3}\eta\, Rh^2(2+\sin^2\psi)\\ (\xi^{MF}_{RR})_{YY} &= \frac{32}{3}\eta\, Rh^2(2+\cos^2\psi)\\ (\xi^{MF}_{RR})_{ZZ} &= \frac{64}{3}\eta\, R^3\end{aligned} \tag{49}$$

and the non-vanishing elements of the coupling blocks are

$$(\xi^{MF}_{RT})_{XX} = -(\xi^{MF}_{RT})_{YY} = (\xi^{MF}_{TR})_{XX} = -(\xi^{MF}_{TR})_{YY} = \frac{32}{3}\eta\, Rh\, \sin\psi\, \cos\psi \tag{50}$$

Notice that the two enantiomers are distinguished only by the opposite sign of the RT (TR) elements. The diffusion matrix is then derived by inverting $\boldsymbol{\xi}^{MF}$. Model calculations have been done for the geometrical parameters indicated in Fig. 4 and for $\eta = 0.01$ Pa s, $T = 300$ K. The non-vanishing elements of the diffusion matrix are listed in Table 3.

We turn now to the parameterization of the orientational potential in the limit $q = 0$. As for the bent-rod molecule, the potential is built as superposition of contributions from the single disks. The general expression of $V_{q=0}(\Omega')$ given for the bent-rod (see eq (45) with eq (46)) still holds. In the present case, the sets of Euler angles to be inserted in eq (46) are $\Omega^{(1)} = (\pi - \psi, \pi/2, 0)$ and $\Omega^{(2)} = (\psi, \pi/2, 0)$, which specify the transformations from MF to local frames tethered to disks I and II, respectively, whose longitudinal axes are perpendicular to the disks' planes. The coefficient $c_0 \equiv c_0^{(1)} = c_0^{(2)} > 0$ here quantifies the

strength of discotic alignment of the two equivalent mojeties with respect to the director. By explicitating the Wigner functions one derives the following expressions for the non-vanishing coefficients for $m = 0, \pm 2$

$$w_{2,m,0}(0) = -d^2_{m,0}(\pi/2)\, c_0$$
$$w_{2,m,\pm 2}(0) = d^2_{m,0}(\pi/2)\, c_0 \sqrt{3/2} \cos 2\psi \qquad (51)$$

The chosen value of c_0 and of the generated order parameters (see eqs (10)) are collected in Table 3.

On the base of such parameterization, $D_{mt}(\mathbf{u}_{hx})$ has been evaluated for the two enantiomers at several values of the pitch. The resulting profiles are shown in Fig. 9, and reveal that the enantiomers are distinguished on the base of their shape chirality. In terms of a pictorial representation, one might think to compare the shape chirality of the propellers with the chirality of the twisted phase, considering that all calculations are referred to a left-handed twisted nematic. The right-handed enantiomer ($\psi = +30°$), having *opposite* chirality with respect to that of the phase, shows again the characteristic monotonic increasing of $D_{mt}(\mathbf{u}_{hx})$ versus the pitch already seen for the ellipsoidal and bent-rod objects. On the contrary, the enantiomer with the *same* chirality of the phase ($\psi = -30°$) shows an increasing profile up to a maximum value in correspondence of an intermediate pitch, and then decreasing towards the asymptotic value (which is the same for both the enantiomers in the untwisted nematic phase). Let us now look at these profiles in the opposite way, that is by reducing the pitch. One can see that twisting the phase slows down the diffusion for the enantiomer $\psi = +30°$, while it speeds up the other one ($\psi = -30°$). In the latter case, such "acceleration" increases up to a maximum as the twist increases; a further twist causes a decreasing of the diffusion coefficient and, below a critic value of the pitch, for both the enantiomers $D_{mt}(\mathbf{u}_{hx})$ is lower than the asymptotic value in the untwisted phase. Finally, notice that the largest difference of $D_{mt}(\mathbf{u}_{hx})$ between the two enantiomers occurs at the shortest pitch, and it is of the order of only $\sim 1.0\%$.

8 Remarks and conclusions

The (macroscopic) diffusion coefficient for a solute moving along the helical axis of the twisted phase, $D_{mt}(\mathbf{u}_{hx})$, has been evaluated for different model molecules of growing complexity, to explore the influence of the local orientational order and of the pitch of the phase.

By considering the simple ellipsoidal molecule as a prototype of elongated mesogens, we have found that an increasing degree of local calamitic order (at fixed pitch) causes a slowdown of the macroscopic diffusion. Moreover, the local biaxiality of the ordering induced by the twist of the director field yields a negligible correction to $D_{mt}(\mathbf{u}_{hx})$ evaluated for uniaxial alignment. The latter outcome suggested us to neglect the local biaxiality in the analysis of the more complex molecular geometries. We also find that reducing the tumbling speed of the particle slows down the translation coefficient $D_{mt}(\mathbf{u}_{hx})$. Calculations regarding the bent-rod molecule, possessing roto-translation coupling in the diffusion matrix but no chirality, revealed a similar behavior of $D_{mt}(\mathbf{u}_{hx})$ versus the pitch as that found for the ellipsoidal molecule.

On the contrary, some new features emerged for the chiral two-disks propeller: the two shape enantiomers respond differently to variations of the pitch. Considering these findings we come back to our main issue of the possibility of separating enantiomers by means of the macroscopic translational diffusion. We have shown that moving in a chiral phase one of the enantiomers is speeded up while the other is slowed down; beyond a critical twist (i.e., below a critical pitch) for both the enantiomers the diffusion is slower than in the untwisted nematic phase but different. We have thus obtained a proof of principle that a separation could be obtained. However, we have shown that the largest differentiation between the propeller-like enantiomers occurs at very low pitch of the order of few tens of molecular lengths, and that it amounts to only $\sim 1.0\%$. It is reasonable to assume that for different parameterizations about the degree of ordering, and for realistic chiral molecules, the order of magnitude of such difference would not change consistently.

It worth to notice here that regardless of the specific kind of molecular architecture, the deviations of $D_{mt}(\mathbf{u}_{hx})$ from the limit value in the nematic phase are substantially of the same order of magnitude for molecules of comparable dimensions (even if the details of the

the profiles in figures 5 - 9 depend on the specific geometrical features). Such a finding can be rationalized with the following argument, based only on scaling properties without accounting for the pitch-dependence of the equilibrium distribution. Let L be a characteristic molecular length; by fixing the viscosity of the medium, the elements of the roto-translational diffusion matrix referred to the Director Frame (DF) scale in simple way according to L: the elements of the TT block are proportional to L^{-1}, those of the RT blocks vary as L^{-2}, and those of the RR block depend on L^{-3}. Accordingly, the function $f(\Omega')$ specified in eq (4) can be expressed as $f(\Omega') = L^{-2}[a+b(L/p)]$, with a and b coefficients dependent on the molecular orientation. Then, the operator in eq (5) is written as $\Gamma'_0 = L^{-3}[(L/p)^2\hat{A}_{TT}+(L/p)\hat{B}_{RT}+\hat{C}_{RR}]$ with $\hat{A}_{TT}$, $\hat{B}_{RT}$ and $\hat{C}_{RR}$ operators acting on the orientational variables. On this basis, consideration of eq (3) leads to predict a dependence $D_{mt}(\mathbf{u}_{hx}) \propto L^{-1}F(L/p)$, where $F(L/p)$ is some (unknown) function of L/p. The factor L^{-1} is intrinsic for translational diffusion coefficients (and essentially it sets their order of magnitude when the viscosity is specified). On the contrary, the factor $F(L/p)$ is the emergent feature when the molecule diffuses in a twisted phase (such a factor approaches to unity when L/p tends to vanish). For a given orientational equilibrium distribution, the specific form of the function F is determined by the structure of the diffusion matrix and by the sign and relative magnitude of its elements (that is, ultimately, by the geometric aspect the molecule). Only full numerical calculations can supply the specific form of function F and this has been, as a matter of fact, our effort in this work. However, with reference to the archetype molecules here considered, it emerges that *i*) the deviation of $F(L/p)$ from unity is mainly determined by the argument L/p itself (i.e., the size of the molecule does matter more than its aspect), and *ii*) the function F depends weakly on L/p. In other words, a relevant feature which affects the magnitude of modulation of the diffusion coefficient is the comparison between molecular size and pitch: quantitative deviations from the limit value in the nematic phase are achieved only if linear extension of the molecule and pitch become comparable.

In particular, this evidence might guide the design of proper phases to be exploited in the discrimination between geometric enantiomers in microdevices. Even if with our model calculations we pointed out that it might be difficult to obtain the separation in practice, recent

development of new short-pitch chiral materials could change the perspective[17, 18] in favor of what is certainly a most important objective. Along this line, we are currently interested in quantifying the degree of discrimination between the enantiomers of helical necklace-like molecules, made of linked spheres, diffusing in a twisted phase of pitch comparable with the molecular length.

9 Acknowledgments

We thank MIUR (PRIN "Liquid Crystals") and INSTM for support. Diego Frezzato also acknowledges the University of Padova for support through "Progetti di Ricerca Giovani Ricercatori 2003", code number CPDG034448.

References

[1] D. Frezzato, C. Zannoni, G. J. Moro, *J. Chem. Phys.* **122**, 164904 (2005).

[2] P. G. de Gennes, P. J. Prost, *The Physics of Liquid Crystals,* 2^{nd} *edition* (Oxford University Press, New York, 1993).

[3] C. W. Gardiner, *Handbook of Stochastic Methods* (Springer, Berlin 1994).

[4] W. A. Wegener, Biopolymers **20**, 303 (1981).

[5] J. Happel and H. Brenner, *Low Reynolds Number Hydrodynamics*, Chap. 5 (Noordhoff, Leyden, 1973).

[6] P. F. Perrin, J. de Physique **7**, 33 (1934); *ibid.*, J. Phys. Radium **5**, 497 (1934); *ibid.*, J. Phys. Radium **7**, 1 (1936).

[7] M. Kostur, M. Schindler, P. Talkner, P. Hänggi, Phys. Rev. Lett. **96**, 014502 (2006).

[8] See EPAPS Document No. ****** for details about the formal tools developed to perform the numerical calculations of the diffusion coefficients in cholesteric phases. The document may be retrieved via the EPAPS homepage (http://www.aip.org/pubservs/epaps.html) or from ftp.aip.org in the directory /epaps/. See the EPAPS homepage for more information.

[9] S. C. Harvey and J. Garcia de la Torre, Macromolecules **13**, 960 (1980); J. Garcia de la Torre. M.C. Lopz Martinez and J.J. Garcia Molina, Macromolecules **20**, 661 (1987).

[10] D. Brune and S. Kim, Proc. Natl. Acad. Sci. USA **90** , 3835 (1993).

[11] M. E. Rose, *Elementary Theory of Angular Momentum* (Wyley, New York, 1957).

[12] R. Berardi and C. Zannoni, J. Chem. Phys., **113**, 5971 (2000)

[13] A. Ferrarini, G. J. Moro, P. L. Nordio, Phys. Rev. E **53**, 681 (1996).

[14] M. Abramowitz, I. A. Stegun, *Handbook of Mathematical Functions* (Dover Publications Inc., New York, 1970).

[15] D. Frezzato, C. Zannoni and G. J. Moro, in preparation.

[16] G. Moro, J. H. Freed, J. Chem. Phys. **74**, 3757 (1981); G. Moro, J. H. Freed, p. 143 in *Large Scale Eigenvalues Problems* (J. Cullum and R. A. Willoughby Eds., Elsevier Science Publishers, North Holland, 1986).

[17] K. Robbie, D. J. Broer and M. J. Brett, Nature **399**, 764 (1999).

[18] Y. Yang, M. Suzuki, H. Fukui, H. Shirai and K. Hanabusa, Chem. Mater. **18**, 1324 (2006).

ELLIPSOID					
order parameters					
$\epsilon/\text{Å}^{-2}$	pitch/Å	$\langle R^2_{0,0}\rangle_{\text{DF}'}$	$\langle R^2_{2,0}\rangle_{\text{DF}'}$	$\langle R^2_{0,2}\rangle_{\text{DF}'}$	$\langle R^2_{2,2}\rangle_{\text{DF}'}$
1.8×10^{-2}	∞	0.6079	0	0	0
	500	0.6071	-7.4×10^{-5}	0	0
3.3×10^{-2}	∞	0.8018	0	0	0
diffusion matrix elements					
$\left(D^{MF}_{TT}\right)_{XX} = \left(D^{MF}_{TT}\right)_{YY} = 2.54 \times 10^{-7}\ \text{cm}^2\,\text{s}^{-1}$					
$\left(D^{MF}_{TT}\right)_{ZZ} = 3.13 \times 10^{-7}\ \text{cm}^2\,\text{s}^{-1}$					
$\left(D^{MF}_{RR}\right)_{XX} = \left(D^{MF}_{RR}\right)_{YY} = 1.88 \times 10^{7}\ \text{s}^{-1}$					
$\left(D^{MF}_{RR}\right)_{ZZ} = 5.88 \times 10^{7}\ \text{s}^{-1}$					

TABLE 1. Parameterization of the elipsoidal molecule employed in the calculation of $D_{mt}(\mathbf{u}_{hx})$.

BENT ROD				
order parameters				
c_0	$\langle R^2_{0,0}\rangle_{\mathrm{DF}'}$	$\langle R^2_{2,0}\rangle_{\mathrm{DF}'}$	$\langle R^2_{0,2}\rangle_{\mathrm{DF}'}$	$\langle R^2_{2,2}\rangle_{\mathrm{DF}'}$
-2.50	0.6060	0	0.03528	0
diffusion matrix elements				
$\left(D^{MF}_{TT}\right)_{XX} = 2.10 \times 10^{-7}\ \mathrm{cm^2\,s^{-1}}$				
$\left(D^{MF}_{TT}\right)_{YY} = 1.86 \times 10^{-7}\ \mathrm{cm^2\,s^{-1}}$				
$\left(D^{MF}_{TT}\right)_{ZZ} = 3.08 \times 10^{-7}\ \mathrm{cm^2\,s^{-1}}$				
$\left(D^{MF}_{RR}\right)_{XX} = 2.39 \times 10^{7}\ \mathrm{s^{-1}}$				
$\left(D^{MF}_{RR}\right)_{YY} = 2.63 \times 10^{7}\ \mathrm{s^{-1}}$				
$\left(D^{MF}_{RR}\right)_{ZZ} = 1.50 \times 10^{8}\ \mathrm{s^{-1}}$				
$\left(D^{MF}_{RT}\right)_{YZ} = \left(D^{MF}_{RT}\right)_{ZY} = -5.81 \times 10^{-1}\ \mathrm{cm\,s^{-1}}$				

TABLE 2. Parameterization of the bent-rod molecule employed in the calculation of $D_{mt}(\mathbf{u}_{hx})$.

SCREW PROPELLERS $\psi = \pm 30^\circ$				
order parameters				
c_0	$\langle R^2_{0,0}\rangle_{\mathrm{DF}'}$	$\langle R^2_{2,0}\rangle_{\mathrm{DF}'}$	$\langle R^2_{0,2}\rangle_{\mathrm{DF}'}$	$\langle R^2_{2,2}\rangle_{\mathrm{DF}'}$
3.90	0.6008	0	-0.08700	0
diffusion matrix elements				
$\left(D^{MF}_{TT}\right)_{XX} = 2.91 \times 10^{-7}\ \mathrm{cm^2\,s^{-1}}$				
$\left(D^{MF}_{TT}\right)_{YY} = 3.56 \times 10^{-7}\ \mathrm{cm^2\,s^{-1}}$				
$\left(D^{MF}_{TT}\right)_{ZZ} = 3.88 \times 10^{-7}\ \mathrm{cm^2\,s^{-1}}$				
$\left(D^{MF}_{RR}\right)_{XX} = 3.56 \times 10^{7}\ \mathrm{s^{-1}}$				
$\left(D^{MF}_{RR}\right)_{YY} = 2.91 \times 10^{7}\ \mathrm{s^{-1}}$				
$\left(D^{MF}_{RR}\right)_{ZZ} = 1.55 \times 10^{8}\ \mathrm{s^{-1}}$				
$\left(D^{MF}_{RT}\right)_{XX} = \mp 5.60 \times 10^{-1}\ \mathrm{cm\,s^{-1}}$				
$\left(D^{MF}_{RT}\right)_{YY} = \pm 5.60 \times 10^{-1}\ \mathrm{cm\,s^{-1}}$				

TABLE 3. Parameterization of the two-disks screw propeller (the two enantiomers) employed in the calculation of $D_{mt}(\mathbf{u}_{hx})$.

FIGURE CAPTIONS

FIG. 1. The employed reference systems of axes: the Molecular Frame (MF), the Laboratory Frame (LF), the Director Frame (DF), and the second director frame (DF'). A left-handed twisted phase is depicted.

FIG. 2. The molecular frame (MF) axes, the location of the Center of Diffusion (CD) and the geometrical parameters for the ellipsoidal (prolate spheroid) molecule.

FIG. 3. The molecular frame (MF) axes, the location of the Center of Diffusion (CD) and the geometrical parameters for the bent-rod molecule.

FIG. 4. The molecular frame (MF) axes, the location of the Center of Diffusion (CD) and the geometrical parameters for the two enantiomers of the screw-propeller molecule.

FIG. 5. Effect of the phase biaxiality induced by the director's twist on the diffusion coefficient along the helical axis. The profiles are referred to the ellipsoidal molecule. Open circles: calculations performed accounting for the twist of the director on the orientational potential. Full circles: calculations performed without accounting for the twist of the director on the orientational potential. See Table 1 for the employed parameters.

FIG. 6. Effect of the order parameter $\overline{P_2} = \langle R^2_{0,0} \rangle_{DF'}$ on the diffusion coefficient along the helical axis. The profiles are referred to the ellipsoidal molecule. The coefficients are scaled with respect to their value at infinite pitch, $D_{mt}(\mathbf{u}_{hx})_\infty$. Open circles: $\overline{P_2} = 0.80$. Open squares: $\overline{P_2} = 0.60$.

FIG. 7. Effect of the slowing down of the rotational motion about the short axes of the ellipsoidal molecule. Full circles: calculations performed with all the diffusion matrix elements in Table 1. Open squares: calculations performed with the $\left(D^{MF}_{RR}\right)_{ZZ}$ given in Table 1 but the transverse rotational diffusion coefficients reduced by a factor 10, i.e.,

$\left(D_{RR}^{MF}\right)_{XX} = \left(D_{RR}^{MF}\right)_{YY} = 1.88 \times 10^6\ \mathrm{s}^{-1}$.

FIG. 8. Pitch dependence of the diffusion coefficient along the helical axis for the bent-rod molecule.

FIG. 9. Pitch dependence of the diffusion coefficient along the helical axis for the two enantiomers of the screw-propeller molecule.

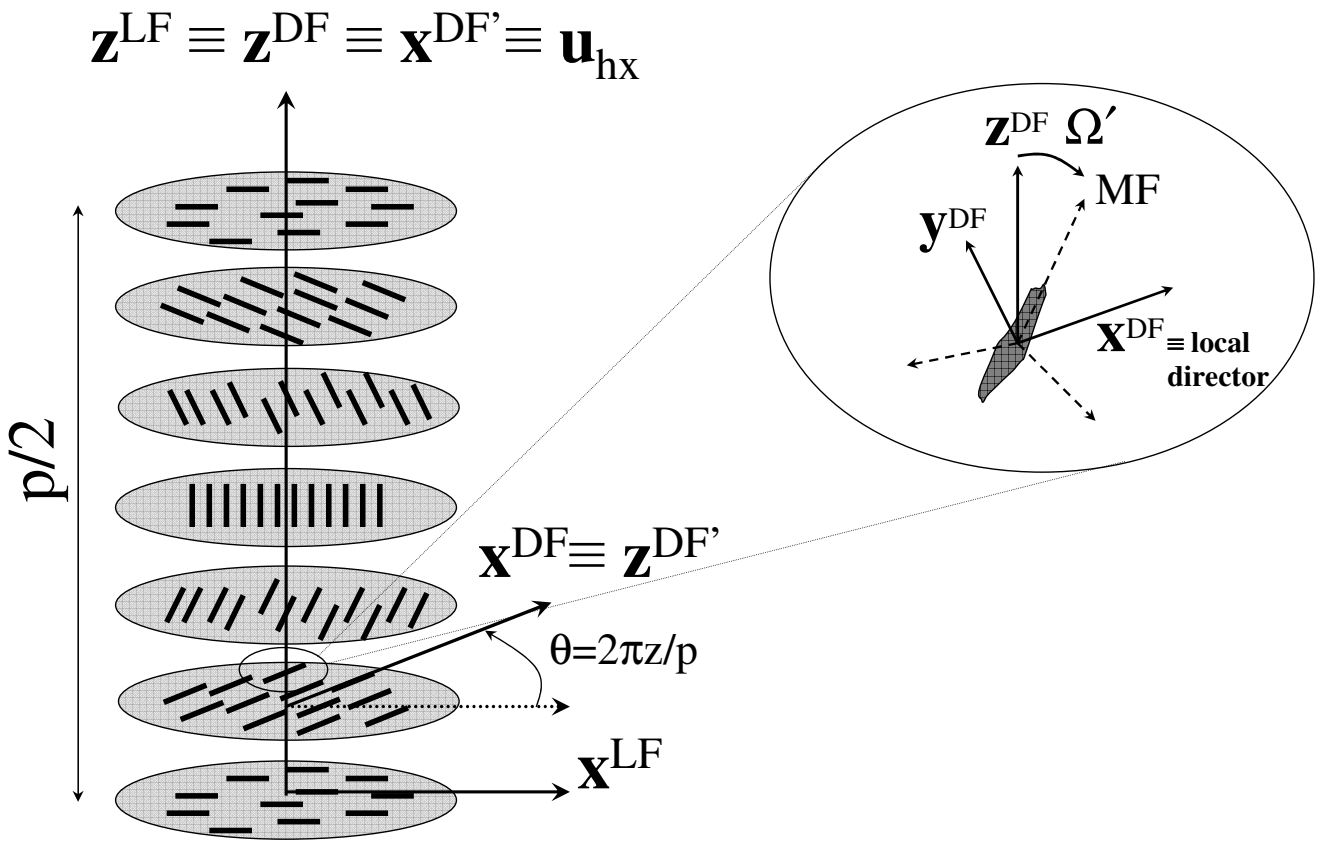
$\mathbf{z}^{LF} \equiv \mathbf{z}^{DF} \equiv \mathbf{x}^{DF'} \equiv \mathbf{u}_{hx}$
p/2
$\mathbf{x}^{DF} \equiv \mathbf{z}^{DF'}$
θ=2πz/p
$\mathbf{x}^{LF}$
$\mathbf{z}^{DF}$ Ω′
MF
$\mathbf{y}^{DF}$
$\mathbf{x}^{DF}$ ≡ local director

FIG. 1

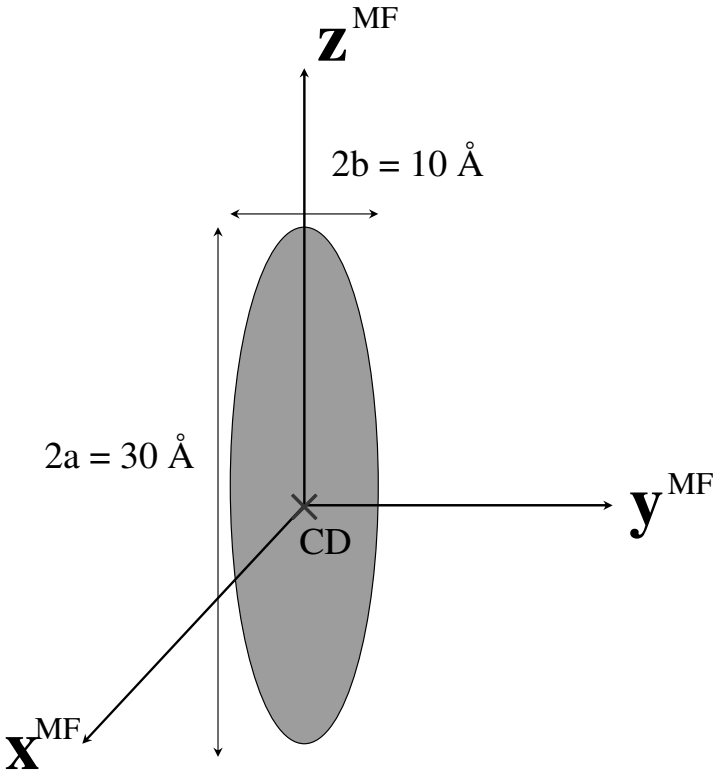

FIG. 2

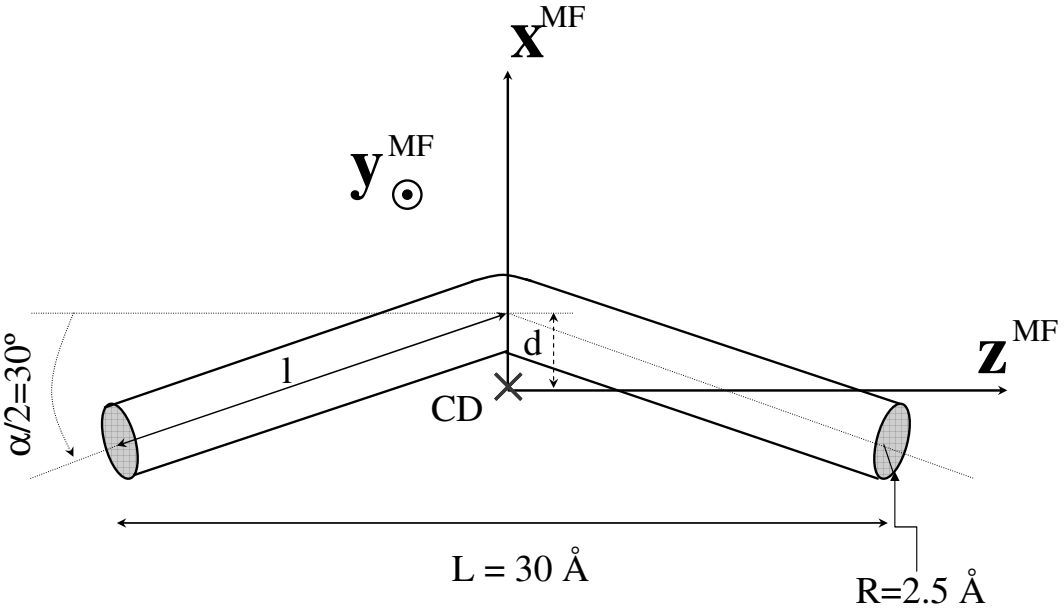

FIG. 3

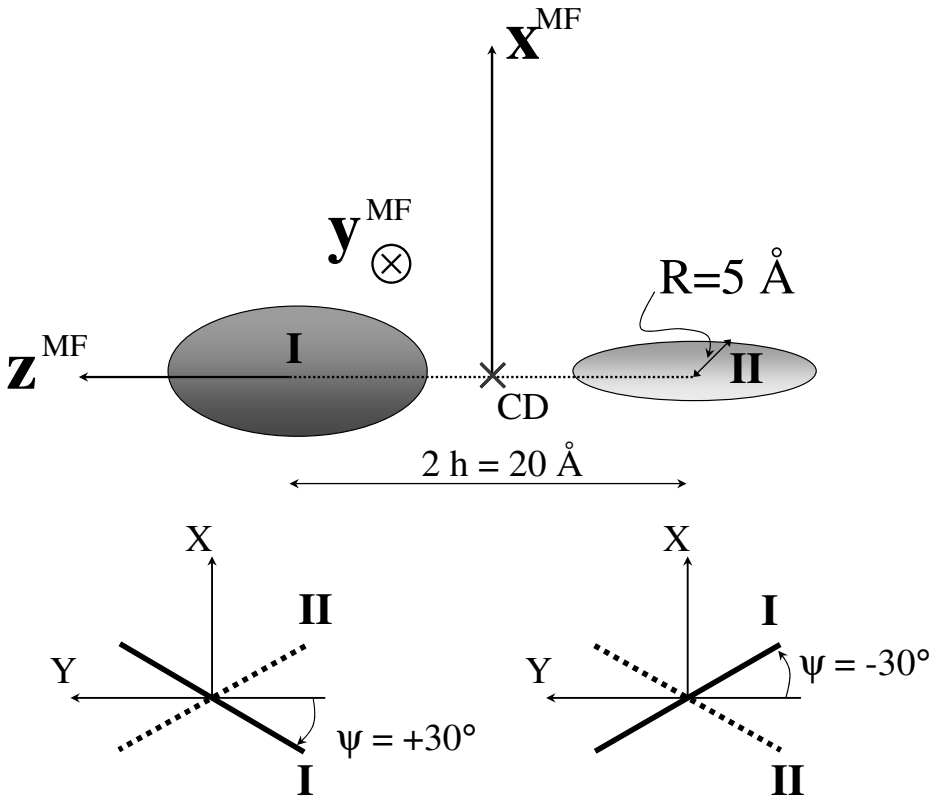

FIG. 4

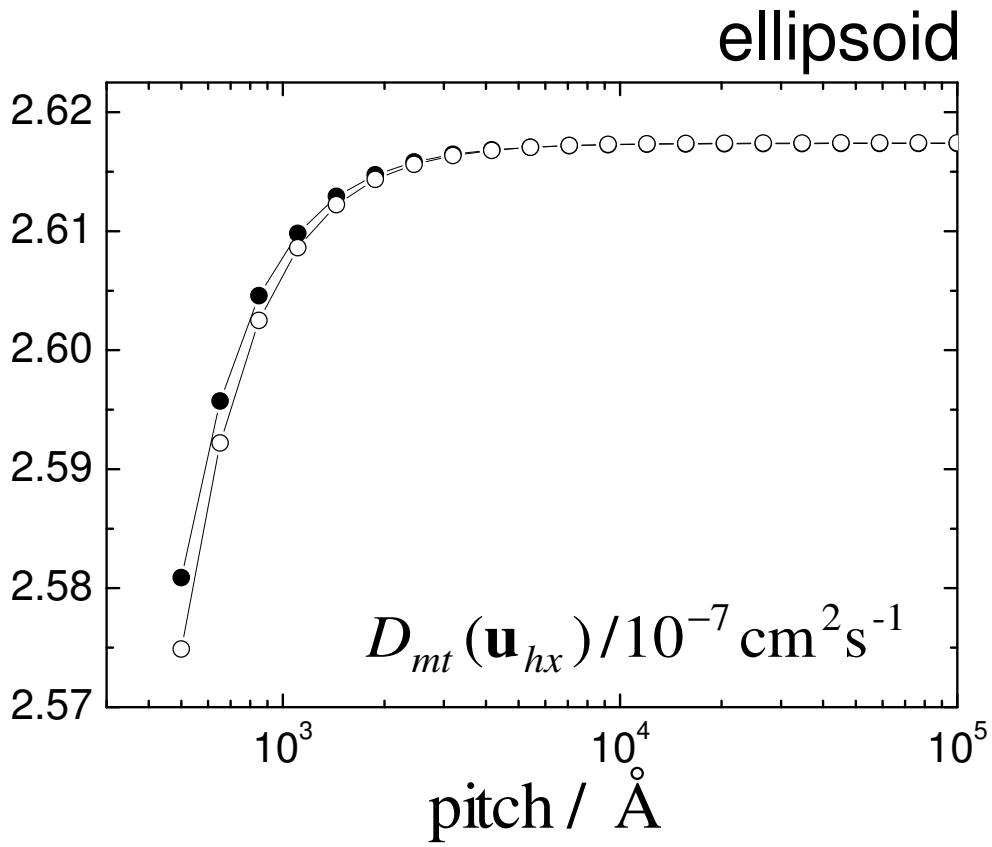
ellipsoid
2.62
2.61
2.60
2.59
2.58
2.57
$D_{mt}(\mathbf{u}_{hx})/10^{-7}\,\mathrm{cm}^2\mathrm{s}^{-1}$
10^3
10^4
10^5
pitch / Å

FIG. 5

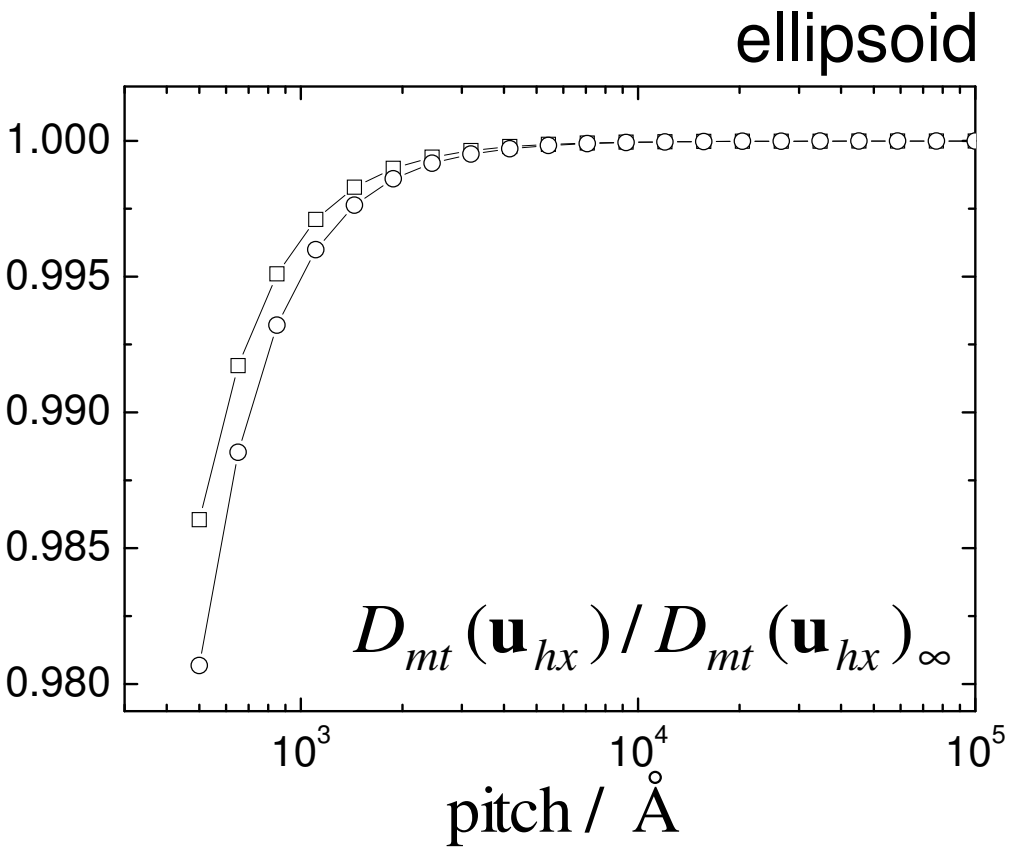
ellipsoid
1.000
0.995
0.990
0.985
0.980
$D_{mt}(\mathbf{u}_{hx}) / D_{mt}(\mathbf{u}_{hx})_{\infty}$
10^3
10^4
10^5
pitch / Å

FIG. 6

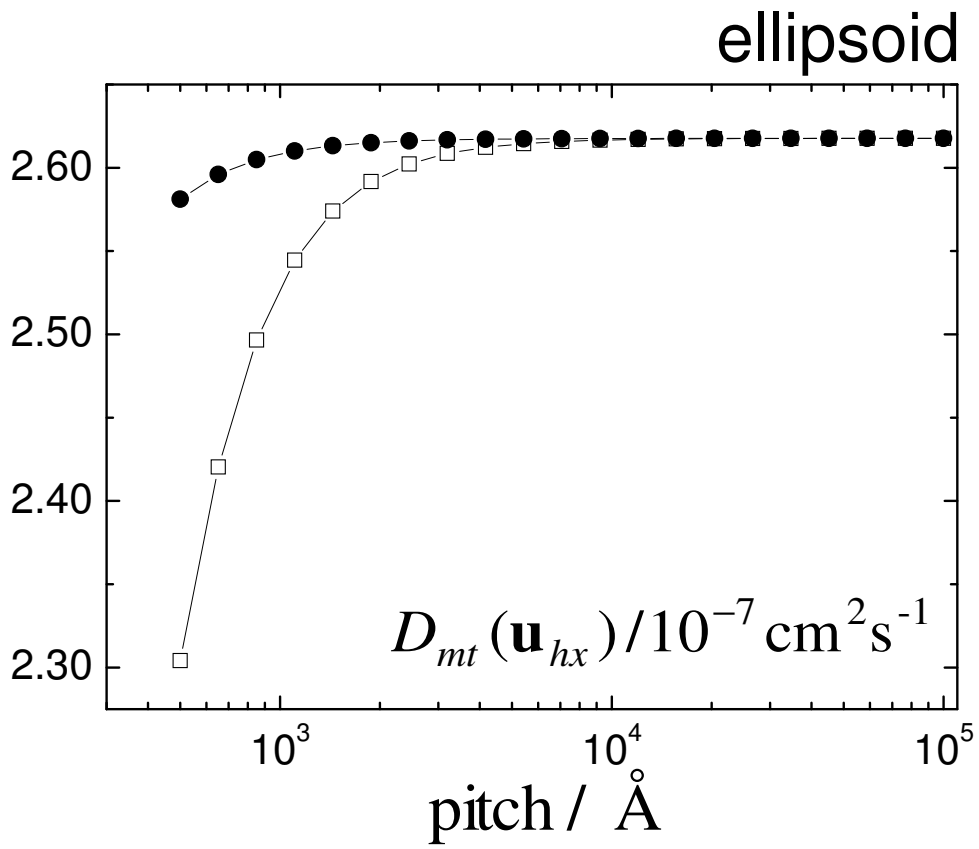
ellipsoid
2.60
2.50
2.40
2.30
$D_{mt}(\mathbf{u}_{hx})/10^{-7}\,\mathrm{cm}^2\mathrm{s}^{-1}$
10^3
10^4
10^5
pitch / Å

FIG. 7

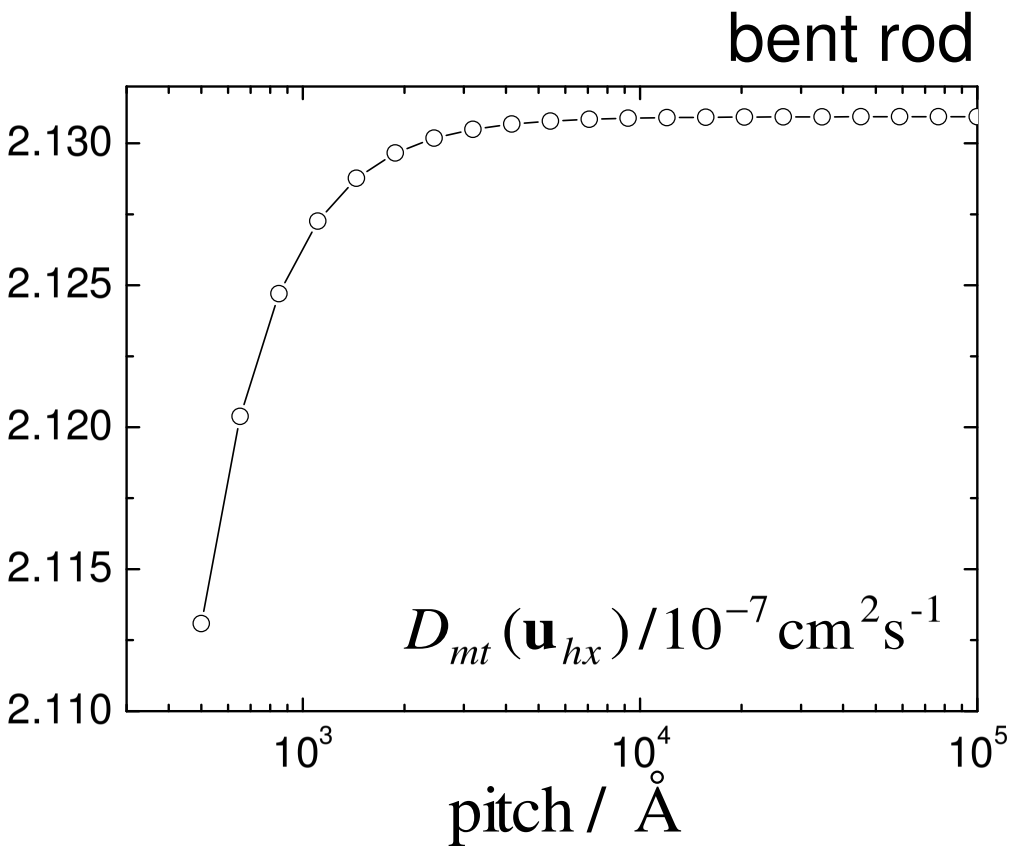
bent rod
2.130
2.125
2.120
2.115
2.110
$D_{mt}(\mathbf{u}_{hx})/10^{-7}\,\mathrm{cm}^2\mathrm{s}^{-1}$
10^3
10^4
10^5
pitch / Å

FIG. 8

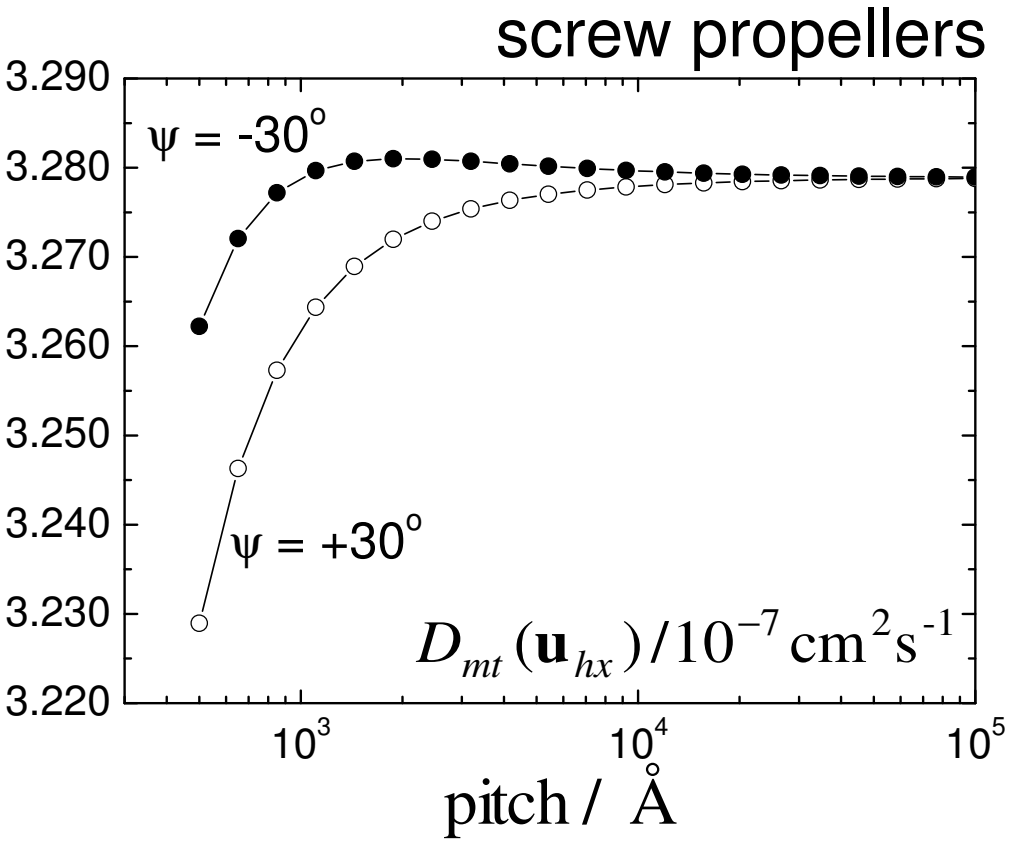
screw propellers
3.290
3.280
3.270
3.260
3.250
3.240
3.230
3.220
ψ = -30°
ψ = +30°
$D_{mt}(\mathbf{u}_{hx})/10^{-7}\,\mathrm{cm}^2\mathrm{s}^{-1}$
10^3
10^4
10^5
pitch / Å

FIG. 9